

# Mycobacterial Protein Tyrosine Phosphatases A and B Inhibitors Augment the Bactericidal Activity of the Standard Anti-tuberculosis Regimen

Noton K. Dutta,<sup>†</sup> Rongjun He,<sup>‡</sup> Michael L. Pinn,<sup>†</sup> Yantao He,<sup>‡</sup> Francis Burrows,<sup>§</sup> Zhong-Yin Zhang,<sup>‡</sup> and Petros C. Karakousis<sup>\*,†,||</sup>

<sup>†</sup>Center for Tuberculosis Research, Department of Medicine, Johns Hopkins University School of Medicine, 1551 East Jefferson Street, Baltimore, Maryland 21287, United States

<sup>‡</sup>Department of Biochemistry and Molecular Biology Indiana University School of Medicine, 635 Barnhill Drive, MS 4053, Indianapolis, Indiana 46202, United States

<sup>§</sup>Aarden Pharmaceuticals, Inc., 351 West 10th Street, Suite 248, Indianapolis, Indiana 46202, United States

<sup>||</sup>Department of International Health, Johns Hopkins Bloomberg School of Public Health, 615 North Wolfe Street, Baltimore, Maryland 21205, United States

## Supporting Information

**ABSTRACT:** Novel drugs are required to shorten the duration of treatment for tuberculosis (TB) and to combat the emergence of drug resistance. One approach has been to identify and target *Mycobacterium tuberculosis* (Mtb) virulence factors, which promote the establishment of TB infection and pathogenesis. Mtb produces a number of virulence factors, including two protein tyrosine phosphatases (PTPs), mPTPA and mPTPB, to evade the antimicrobial functions of host macrophages. To assess the therapeutic potential of targeting the virulent Mtb PTPs, we developed highly potent and selective inhibitors of mPTPA (L335-M34) and mPTPB (L01-Z08) with drug-like properties. We tested the bactericidal activity of L335-M34 and L01-Z08 alone or together in combination with the standard anti-tubercular regimen of isoniazid–rifampicin–pyrazinamide (HRZ) in the guinea pig model of chronic TB infection, which faithfully recapitulates some of the key histological features of human TB lesions. Following a single dose of L335-M34 50 mg/kg and L01-Z08 20 mg/kg, plasma levels were maintained at levels 10-fold greater than the biochemical IC<sub>50</sub> for 12–24 h. Although neither PTP inhibitor alone significantly enhanced the antibacterial activity of HRZ, dual inhibition of mPTPA and mPTPB in combination with HRZ showed modest synergy, even after 2 weeks of treatment. After 6 weeks of treatment, the degree of lung inflammation correlated with the bactericidal activity of each drug regimen. This study highlights the potential utility of targeting Mtb virulence factors, and specifically the Mtb PTPs, as a strategy for enhancing the activity of standard anti-TB treatment.

**KEYWORDS:** *Mycobacterium tuberculosis*, protein tyrosine phosphatases, inhibitors, pharmacokinetics, rifampin, isoniazid, pyrazinamide, chemotherapy, bactericidal, sterilizing, activity, guinea pig, virulence factors

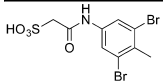
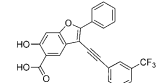
*Mycobacterium tuberculosis* (Mtb) is the causative agent of tuberculosis (TB), which infects a third of the world's population, causing between 1.2 and 2 million deaths annually.<sup>1</sup> Although curative drug regimens are available, such therapy is onerous, and the emergence of HIV/AIDS has triggered a resurgence of TB.<sup>2</sup> A major obstacle to TB eradication efforts is antibiotic resistance, due primarily to inadequate adherence to the treatment regimen, which is complex, requiring multiple drugs for a minimum of 6 months. Multi-drug-resistant (MDR) TB now affects over 50 million people, with an increasing number of cases of extensively drug-resistant (XDR) TB, which carries high mortality rates due to limited treatment options.<sup>3</sup> The prevalence of MDR and XDR TB and the ongoing AIDS epidemic highlight the need to identify new drug targets and develop innovative strategies to combat drug-susceptible and

drug-resistant TB.<sup>4</sup> Recent work has focused on identifying and targeting pathogen virulence factors, which promote the establishment of infection and TB-related pathogenesis.<sup>5,6</sup>

Protein tyrosine phosphatases (PTPs) constitute a large family of signaling enzymes that, together with protein tyrosine kinases (PTKs), modulate the proper cellular level of protein tyrosine phosphorylation.<sup>7,8</sup> Malfunction of either PTKs or PTPs results in aberrant protein tyrosine phosphorylation, which has been linked to the etiology of many human diseases, including cancer, diabetes, and immune dysfunction.<sup>9</sup> The importance of PTPs in cellular physiology is further

Received: November 4, 2015

Table 1. Molecular and Cellular Properties of Lead mPTPA and mPTPB Inhibitors

Structure	Name	Target	Biochemical potency against target (IC <sub>50</sub> , nM)		Fold selectivity		In vitro anti-Mtb activity (uM)	
			mPTPA	mPTPB	vs. mPTPA/B	vs. PTP panel <sup>a</sup>	MABA-MIC <sup>b</sup> H37Rv Erdman	Mtb-infected macrophages <sup>c</sup>
	L335M34	mPTPA	160	>3200	>20	>20	>10 >10	1.38
	L01Z08	mPTPB	2500	38	66	>37	>10 >10	<5

<sup>a</sup>Human PTP panel: PTP1B, TC-PTP, SHP1, SHP2, FAP1, Lyp, Meg2, HePTP, laforin, VHX, VHR, LMWPPTP, Cdc14A, PTP $\alpha$ , LAR, CD45, PTPRG. <sup>b</sup>MABA-MIC = microplate Alamar Blue assay for minimum inhibitory concentration. <sup>c</sup>IC<sub>90</sub> in macrophages activated with interferon- $\gamma$ .

underscored by the fact that they are often exploited and subverted by pathogenic bacteria to cause infection. The PTPs mPTPA and mPTPB from Mtb are required for optimal bacillary survival within host macrophages<sup>10–14</sup> and in animal models.<sup>10,15</sup> Although Mtb itself lacks endogenous protein tyrosine phosphorylation, mPTPA and mPTPB support Mtb infection by acting on macrophage proteins to modulate host–pathogen interactions. Specifically, mPTPA prevents phagolysosome acidification by dephosphorylation of its substrate, Human Vacuolar Protein Sorting 33B,<sup>16</sup> resulting in the exclusion of the macrophage vacuolar-H<sup>+</sup>-ATPase (V-ATPase) from the vesicle.<sup>17</sup> We previously reported that once inside the macrophage, mPTPB activates Akt signaling and simultaneously blocks ERK1/2 and p38 activation to prevent host macrophage apoptosis and cytokine production.<sup>13</sup> Importantly, deletion of mPTPA or mPTPB decreases Mtb survival within interferon- $\gamma$  (IFN- $\gamma$ )-activated macrophages and severely reduces the Mtb bacillary load in the lungs of chronically-infected guinea pigs.<sup>10,18</sup> Moreover, Mtb recombinant strains deficient in PTP activity were found to protect guinea pigs against challenge with virulent Mtb.<sup>15</sup> The finding that mPTPA and mPTPB mediate Mtb survival within macrophages by targeting host cell processes<sup>12,14,15</sup> led to the hypothesis that specific inhibition of their phosphatase activity may augment intrinsic host signaling pathways to eradicate TB infection. To this end, we and others have shown that small-molecule mPTPB inhibitors are capable of reversing the altered host immune responses induced by the bacterial phosphatase and impairing Mtb survival in macrophages, validating the concept that chemical inhibition of mPTPB may be useful for TB treatment.<sup>19,20</sup>

In the current study, we describe the design, synthesis, and characterization of the most potent and selective inhibitor for mPTPA. We then report the evaluation of the bactericidal activity of specific mPTPA and mPTPB inhibitors, either alone or as a cocktail, in combination with the standard regimen of isoniazid–rifampicin–pyrazinamide (HRZ) in a well-validated chronic TB infection model in guinea pigs. Pharmacokinetic studies were performed to establish clinically relevant doses of each inhibitor. Therapeutic efficacy was assessed by the change in lung mycobacterial load and pathology. The public health significance of this research lies in the development of a novel class of agents for more effective treatment of drug-susceptible and drug-resistant TB.

## RESULTS AND DISCUSSION

**Development of Potent and Selective mPTPA and mPTPB Inhibitors.** Therapeutic targeting of PTPs has historically been stalled by difficulties in achieving inhibitor selectivity and bioavailability. The highly conserved PTP active site presents considerable challenges in obtaining compounds that can selectively inhibit the target of interest without adversely hitting other PTPs. In order to accommodate phospho-substrates, the PTP active site is positively charged, which favors negatively charged molecules in high-throughput screening campaigns that suffer from poor cell membrane permeability. To address the selectivity issue, we have pioneered a novel paradigm for the acquisition of potent and selective PTP inhibitors by targeting both the PTP active site and unique pockets in the vicinity of the active site.<sup>21,22</sup> To address the bioavailability issue, we sought to explore the existing natural product and FDA-approved drug space for previously unknown PTP inhibitory activities since these molecules already possess acceptable pharmacological properties. We previously identified benzofuran salicylic acid as a privileged pharmacophore for mPTPB.<sup>13</sup> Using a fragment-based medicinal chemistry approach, we transformed the benzofuran salicylic acid core into a highly potent and selective mPTPB inhibitor (L01-Z08, Table 1) with excellent in vivo efficacy.<sup>20</sup>

More recently, we discovered that cefsulodin, a third generation cephalosporin  $\beta$ -lactam antibiotic, exhibits inhibitory activity against a number of PTPs.<sup>23</sup> Fragmentation analysis of cefsulodin identified  $\alpha$ -sulfophenylacetic amide (SPAA) as an mPTP-inhibiting pharmacophore and a novel pTyr mimetic. Structure-guided and fragment-based optimization of SPAA led to compound L335-M34, which displayed an IC<sub>50</sub> value of 160 nM for mPTPA (Table 1). Kinetic analysis revealed that L335-M34 is a reversible and competitive inhibitor of mPTPA with a  $K_i$  of  $56 \pm 2.0$  nM (Figure 1). To determine the specificity of L335-M34, we measured its inhibitory activity toward mPTPB and a panel of mammalian PTPs, including cytosolic PTPs, PTP1B, TC-PTP, SHP1, SHP2, FAP1, Lyp, PTP-Meg2, and HePTP, the receptor-like PTPs, PTP $\alpha$ , LAR, CD45, and PTPRG, the dual specificity phosphatases VHR, Laforin, VHX, and Cdc14A, and the low molecular weight PTP. As shown in Table 1, L335-M34 is highly selective for mPTPA, exhibiting greater than 20-fold selectivity over all PTPs examined. To the

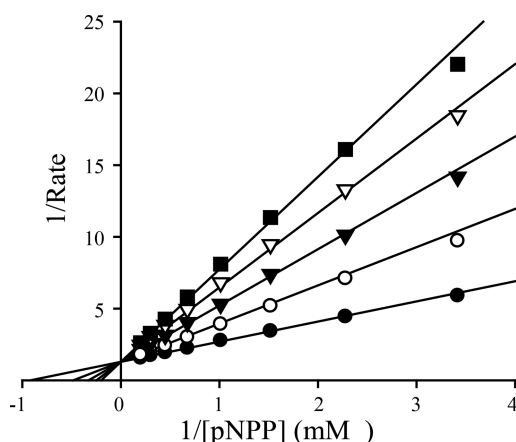


**Figure 1.** Compound L335-M34 is a reversible and competitive inhibitor of mPTPA with pNPP as a substrate. Lineweaver–Burk plot for L335-M34-mediated mPTPA inhibition. Compound L335-M34 concentrations were 0 (●), 50 (○), 100 (▽), 150 (▼), and 200 nM (■). The  $K_i$  value of  $56 \pm 2.0$  nM was determined from three independent measurements.

best of our knowledge, L335-M34 represents the most potent and specific mPTPA inhibitor reported to date.<sup>24–27</sup>

**Cellular Activity of mPTPA and mPTPB Inhibitors L335-M34 and L01-Z08.** The mPTPA inhibitor L335-M34 is highly selective for its target, with an  $IC_{50}$  of 160 nM against mPTPA but no significant activity against mPTPB or a panel of human PTPs at concentrations below 3  $\mu$ M. Because mPTPA is a secreted virulence factor that regulates host antibacterial responses rather than Mtb physiology,<sup>28</sup> it was unsurprising that L335-M34 was devoid of activity in standard MIC assays; however, the compound was able to markedly decrease bacterial load in Mtb-infected macrophages at low micromolar concentrations (Table 1).

The L01 family comprises three highly active and selective mPTPB inhibitors.<sup>20</sup> The selected lead compound from this series, L01-Z08, displayed a potency of 38 nM against mPTPB and was 66-fold less potent against mPTPA and at least 37-fold selective when screened against a panel of 17 human PTPs. Like the mPTPA inhibitor L335-M34, L01-Z08 was inactive in the MIC assay but displayed potent anti-Mtb activity in J774A.1 macrophages (Table 1).

**mPTPA and mPTPB Inhibitors Are Bioavailable and Well-Tolerated in Guinea Pigs Following Oral Dosing.** As shown in Figure 2, L01-Z08 and L335-M34 showed good oral bioavailability and half-life in guinea pigs (Table 2). Both drugs were rapidly absorbed, reaching peak concentrations within a few hours with a typical biphasic plasma clearance curve. Because the drugs were to be coformulated for oral delivery in the therapy study, a combination PK study was performed to confirm that they were amenable to coadministration. Coformulating L01-Z08 with L335-M34 in a single dosing solution did not negatively affect uptake or clearance of either drug. In fact, the bioavailability of L335-M34 was affected only moderately; a slight increase in uptake rate led to a greater peak concentration, which was offset by somewhat more rapid clearance, so that the overall exposure ( $AUC_{ALL}$ ) was essentially unchanged. By contrast, L01-Z08 exposure was enhanced by coadministration (both  $C_{max}$  and beta-phase  $T_{1/2}$  were elevated), but a reduction in the volume of distribution suggested that drug delivery to the tissues was probably not improved (Table 2). The PK study strongly indicated that the

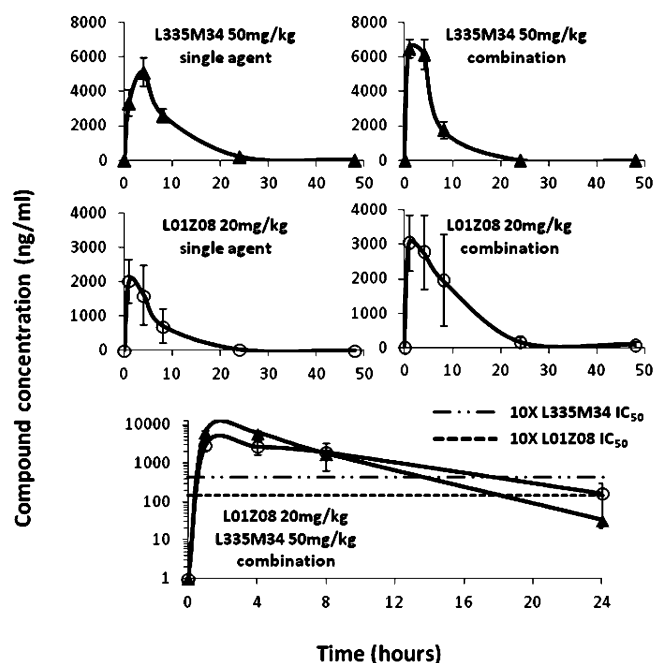


**Figure 2.** Pharmacokinetic profile of lead mPTP inhibitors in guinea pig plasma. Concentration of mPTP inhibitors in the plasma over time. L335-M34 (mPTPA) 50 mg/kg or L01-Z08 (mPTPB) 20 mg/kg was given orally once alone or in combination, and blood samples were collected at the indicated intervals relative to dosing.  $N = 3$  per time point; graph represents mean  $\pm$  SD values.

two compounds could be delivered with adequate efficiency in the guinea pig by the oral route. As shown in the bottom panel of Figure 2, at the doses selected for use in the efficacy study, L335-M34 and L01-Z08 were detected at concentrations 10-fold in excess of their biochemical  $IC_{50}$  values for 12–14 and 20–24 h, respectively, suggesting that once daily oral dosing was an appropriate schedule for each drug. However, it should be noted that a higher degree of selectivity for these compounds was observed in the biochemical assays ( $IC_{50}$ ) than in the whole-cell assays in macrophages (growth inhibition/ $IC_{90}$ ), perhaps due to cell permeability issues.<sup>29</sup>

Guinea pigs receiving L01-Z08 20 mg/kg and L335-M34 50 mg/kg once daily alone or in combination for 6 weeks showed no overt signs of toxicity and displayed similar mean weight gain to those receiving HRZ (Figure S1). All guinea pigs receiving L01-Z08 and L335-M34 survived and gained weight throughout the course of the efficacy study.

**Dual Inhibition of mPTPA and mPTPB Significantly Reduces Guinea Pig Lung Bacillary Burden Relative to HRZ Alone.** Since each mPTP modulates distinct Mtb clearance pathways in macrophages, we hypothesized that dual inhibition of mPTPA and mPTPB would enhance the bactericidal activity of the standard antitubercular regimen in guinea pigs more than adjunctive therapy with either agent alone. Following aerosol infection of guinea pigs with Mtb H37Rv,  $2.06 \pm 0.15 \log_{10}$  bacilli were deposited in the lungs on day –27, and the organisms multiplied to a peak burden of  $6.11 \pm 0.15 \log_{10}$  CFU (colony-forming units) on day 0 (time of treatment initiation). Thereafter, bacillary growth was controlled in the lungs of untreated guinea pigs, which had  $5.82 \pm 0.17 \log_{10}$  CFU in the lungs at the conclusion of the study.

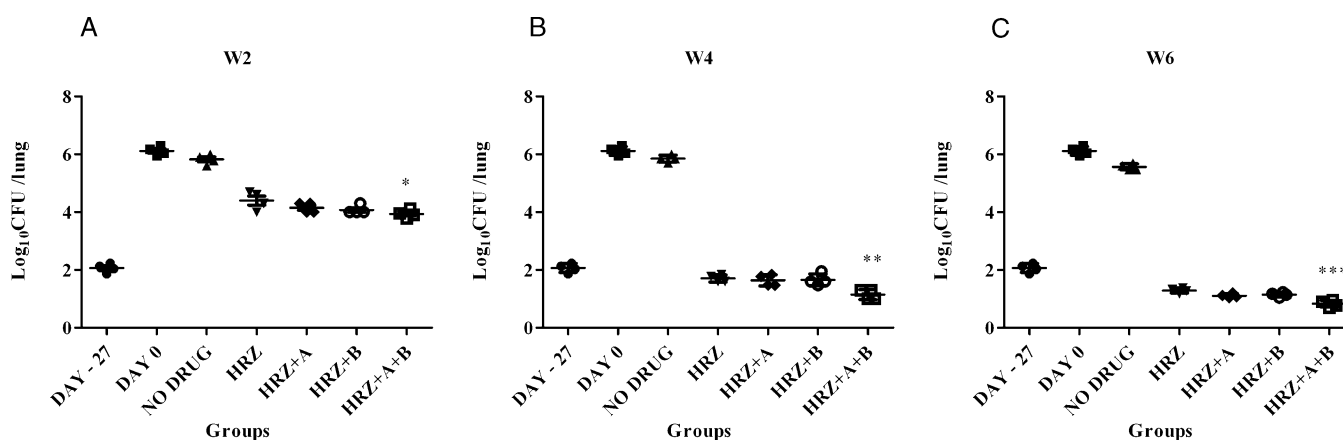
Following 2 weeks of treatment, all guinea pigs in the HRZ, HRZ+L335-M34 (A), HRZ+L01-Z08 (B), and HRZ+AB

Table 2. Pharmacokinetics of mPTPA and mPTPB Inhibitors in Guinea Pigs<sup>a</sup>

compound	dose type	AUC <sub>ALL</sub> (h·ng/mL)	clearance (mL/h/kg)	C <sub>max</sub> (ng/mL)	T <sub>max</sub> <sup>b</sup> (h)	half-life (h)	V <sub>D</sub> <sup>c</sup>
L335M34	single	54406.61	917.462	5142.47	2.5	5.197	6878.467
L335M34	coadmin <sup>d</sup>	52752.61	950.034	7064.956	2.5	4.16	5702.19
L01Z08	single	13166.89	1518.474	1870.43	1.587	5.512	12074.939
L01Z08	coadmin <sup>d</sup>	28161.76	701.564	3059.668	1.587	6.141	6215.132

<sup>a</sup>Data represent mean values for 2–3 animals. <sup>b</sup>T<sub>max</sub> is the time required to achieve the maximal concentration (C<sub>max</sub>). <sup>c</sup>Volume of distribution.

<sup>d</sup>Both compounds L335M34 (50 mg/kg) and L01Z08 (20 mg/kg) were coadministered orally.



**Figure 3.** Activity of adjunctive mPTPA and mPTPB inhibitors against chronic TB infection in guinea pigs. Animals were infected via aerosol with  $\sim 10^2$  CFU of *M. tuberculosis* H37Rv and were either left untreated or were treated with drugs beginning 4 weeks after infection. Log<sub>10</sub> CFU in the lungs are shown after 2 (A), 4 (B), and 6 (C) weeks of treatment. No drug = untreated, HRZ: isoniazid (H), 60/rifampin (R), 100/pyrazinamide (Z), 300; mPTPA/A: L335-M34, 50; mPTPB/B: L01-Z08, 20; numbers after each drug refer to doses (mg/kg);  $n = 4$  guinea pigs per time point; \* $p < 0.05$ , \*\* $p < 0.01$ , \*\*\* $p < 0.001$ , HRZ versus HRZ+A+B.

groups were able to contain Mtb multiplication in the lungs, resulting in mean bacillary burdens of  $4.44 \pm 0.31$ ,  $4.07 \pm 0.15$ ,  $4.15 \pm 0.17$ , and  $3.77 \pm 0.21$  log<sub>10</sub>, respectively. After 2 weeks of treatment, lung CFU counts in animals treated with HRZ+AB were significantly ( $p < 0.01$ ) lower than those treated with HRZ (Figure 3A). However, no significant differences were observed in lung CFU between HRZ+A, HRZ+B, and HRZ+AB.

At 4 weeks post-treatment, a similar trend was seen and the hierarchy of bactericidal activities of the various regimens was HRZ+AB ( $1.15 \pm 0.17$  log<sub>10</sub> CFU) > HRZ+B ( $1.64 \pm 0.19$  log<sub>10</sub> CFU) > HRZ+A ( $1.65 \pm 0.2$  log<sub>10</sub> CFU) > HRZ ( $1.70 \pm 0.12$  log<sub>10</sub> CFU) (Figure 3B). HRZ+AB was significantly more active than HRZ+B, HRZ+A, and HRZ alone ( $p < 0.001$ ).

After 6 weeks of treatment, HRZ reduced mean lung CFU by  $4.27$  log<sub>10</sub> compared to untreated controls (Figure 2C). The addition of L335-M34 (A) or L01-Z08 (B) to the standard regimen further reduced mean lung CFU by  $0.14$  log<sub>10</sub> and  $0.17$  log<sub>10</sub>, respectively, and the combination (AB) lowered mean lung CFU by  $0.45$  log<sub>10</sub> ( $p < 0.0001$ ) relative to HRZ (Figure 3C).

The gross pathology of guinea pig lungs (data not shown), as well as mean guinea pig lung and spleen weights (Figure S2), correlated with the efficacy of the various chemotherapy regimens. Interestingly, the mean lung surface area involved by inflammation after 6 weeks of treatment was significantly lower in the HRZ+AB (9.23%) group relative to the HRZ group (36.28%) ( $p = 0.028$ ). Our results suggest that this effect on improved histopathology is primarily conferred by inhibition of mPTPA (HRZ+A vs HRZ+AB,  $p = 0.68$ ) (Figure 4 and Figure S3).

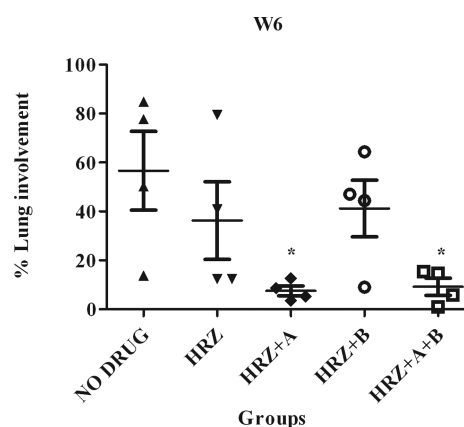


**Figure 4.** Lung inflammation 6 weeks after initiation of treatment. Results are represented as percentage of lung surface area involved, calculated using ImageJ software. Compared to HRZ, HRZ+A/HRZ+A+B are more effective in reducing lung lesion size and number in *M. tuberculosis*-infected guinea pigs at month 1.5 after treatment; \* $p < 0.05$ , HRZ versus HRZ+A/HRZ+A+B.

Our fragment-based lead optimization strategies have yielded two compounds, L01-Z08 and L335-M34, with potent activity against intracellular Mtb, as well as favorable PK and toxicity profiles. L01-Z08 and L335-M34 are inhibitors of the key secreted Mtb enzymes, mPTPB and mPTPA, respectively, and thus provide a novel mechanism of action for the treatment of TB. Both phosphatases are secreted by Mtb into the cytoplasm of the macrophage and are important for persistence of mycobacterial infection.<sup>10,30</sup> In order to determine the potential for translation of our findings to the clinical arena, we evaluated whether mPTP inhibitors could be beneficial as an adjunctive



treatment when combined with the standard first-line regimen against drug-susceptible TB in guinea pigs. The two mPTPA and mPTPB inhibitor lead compounds showed promising oral bioavailability and tolerability in this model. Although each inhibitor alone added little bactericidal activity to the standard regimen, dual inhibition of mPTPA and mPTPB significantly reduced the lung bacillary burden relative to HRZ at each time point studied.

PTKs are the molecular targets for a growing number of anticancer agents;<sup>31</sup> however, there is a notable absence of drugs targeting the PTPs. Although many disease-relevant pathways are also controlled by PTPs,<sup>32–34</sup> the latter have proven to be exceptionally challenging targets for the development of new therapeutic agents,<sup>34</sup> due primarily to the poor bioavailability of existing PTP inhibitory compounds. The observed oral bioavailability and in vivo efficacy of L01-Z08 and L335-M34 are promising and further demonstrate that it is feasible to obtain PTP inhibitors that are sufficiently polar to bind the active site and yet still possess favorable pharmacological properties for therapeutic development.

Given the unique mechanisms of action of the mPTPA and mPTPB inhibitors, these compounds are expected to provide additive bactericidal activity to the standard regimen for drug-susceptible TB as well as to novel regimens for drug-resistant TB. Moreover, concomitant treatment with such inhibitors may reduce the risk for selection of strains resistant to currently available anti-TB drugs during treatment.<sup>8</sup> Previous work has shown that small-molecule inhibitors of both mPTPA and mPTPB are capable of reducing intracellular mycobacteria in infected macrophages.<sup>8,13,35</sup> It is interesting to note that adjunctive inhibition of mPTPA led to improved lung histopathology relative to standard treatment alone. A recent study showed that mPTPA dephosphorylates a second substrate, glycogen synthase kinase- $\alpha$  (GSK- $\alpha$ ), causing its activation and the subsequent inhibition of the cell death program in infected macrophages.<sup>35</sup> Based on available data, dual inhibition of mPTPA and mPTPB appears to undermine Mtb infection by (i) increasing intracellular destruction of bacteria,<sup>36</sup> (ii) promoting host-beneficial apoptosis of infected macrophages,<sup>13</sup> and (iii) increasing host immunologic awareness of, and responsiveness to, Mtb infection.<sup>8,35</sup>

Previous studies<sup>37</sup> have indicated that mPTPA is not essential for Mtb survival in mice, implying that the murine model fails to recapitulate the phenotypes reported in human macrophages.<sup>16</sup> Although the mouse model has long been used to evaluate TB drugs,<sup>38</sup> it has been increasingly recognized in the TB field that observations made in mice are not predictive of treatment outcomes in human clinical trials, nor is early “sterilization” a predictor of cure.<sup>39,40</sup> In the current study, we used the well-characterized guinea pig model of TB chemotherapy.<sup>41–48</sup> Compared to mice, guinea pig TB granulomas more closely approximate their human counterparts with respect to cellular composition, granuloma architecture, and the presence of caseation necrosis.<sup>49</sup> In addition, tissue hypoxia is present in guinea pig TB granulomas<sup>46,50</sup> but absent in mouse TB lung lesions.<sup>51,52</sup> These histological and micro-environmental factors, which may be biological determinants of Mtb persistence,<sup>53</sup> as well as concordance of treatment outcomes with those of recent human studies,<sup>39,54</sup> make the guinea pig model an attractive one for testing the activity of novel anti-tubercular agents.<sup>41–44,46,47</sup> However, the anti-tubercular activity of these agents could be further characterized

in other clinically relevant models, such as the rabbit and non-human primate.

Our study contains several limitations. Considering the robust anti-tubercular activity of the mPTP inhibitors in macrophages, the corresponding activity of these agents against Mtb in guinea pig lungs was relatively modest. One potential explanation for this is reduced drug bioavailability at the site of infection. Although plasma levels of each inhibitor were determined after oral dosing, we did not directly measure drug concentrations in the lung lesions. Using MALDI-TOF, Prideaux et al. showed that the anti-tubercular activity of moxifloxacin may be limited due to inadequate penetration into necrotic granulomas in rabbits.<sup>55,56</sup> As suggested by the discrepancy between the biochemical IC<sub>50</sub> values of each agent and their corresponding IC<sub>90</sub> values against intracellular Mtb, the entry of these compounds into macrophages may be somewhat limited. In addition, we have shown previously that a large population of bacilli is found in the extracellular compartment of necrotic lung granulomas in guinea pigs.<sup>43</sup> Based on their mechanism of action, mPTP inhibitors would likely have no activity against such organisms. Finally, it is possible that functional deficiency of mPTPA and/or mPTPB may be compensated by alternative Mtb phosphatases, such as SapM.<sup>15</sup> Recently, Chauhan et al. generated an Mtb mutant (Mtb $\Delta$ mms) by disrupting the genes encoding PtpA, PtpB, and SapM. After 10 weeks of infection, guinea pigs infected with Mtb $\Delta$ mms showed a 4.69 log<sub>10</sub> reduction in lung CFU relative to those infected with the isogenic wild-type strain.<sup>15</sup> This mutant was more attenuated in the guinea pig model of chronic TB relative to an Mtb mutant lacking only mPTPB.<sup>10</sup> Future studies will focus on dose optimization, taking into account both plasma and tissue concentrations of mPTP inhibitors. In addition, we will attempt to identify potent inhibitors of Mtb SapM, which can be coformulated with mPTPA and mPTPB inhibitors.

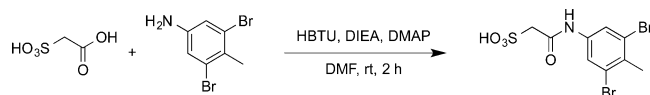
Our data support the further development of the Mtb PTP inhibitor class of drugs. We showed that PTP inhibitors lack direct antimicrobial activity but promote intracellular Mtb killing in vitro. Our findings suggest a modest increase in killing by the standard regimen with dual mPTPA/B inhibition, as well as a favorable PK interaction between the agents. Significantly, our data suggest that PTP inhibitors may improve clinical outcomes by ameliorating lung pathology. Further studies are needed to better characterize the sterilizing activity of these agents and their potential for improving TB-induced lung pathology.

## ■ MATERIALS AND METHODS

### General Procedures for the Preparation of Inhibitors.

Reagents were used as purchased from Sigma-Aldrich and Fisher Scientific. <sup>1</sup>H and <sup>13</sup>C NMR spectra were obtained on a BrukerAvance II 500 MHz NMR spectrometer with tetramethylsilane or residual solvent as standard. Mass spectra were obtained using an Agilent Technologies 6130 quadrupole LC/MS. HPLC purification was carried out on a Waters Delta 600 equipped with a Sunfire Prep C18 OBD column (30 mm/150 mm, 5  $\mu$ m) with methanol–water (both containing 0.1% TFA) as the mobile phase (gradient: 50–100% methanol, flow 10 mL/min). The purity of all final tested compounds was established to be >95% by Agilent Technologies 6130 quadrupole LC/MS by using methanol–water (both containing 0.1% TFA) as the mobile phase (gradient: 0–100% methanol,

flow 1.0 mL/min), with UV monitoring at the fixed wavelength of 254 nm.



**Synthesis of L335-M34 (mPTPA).** To a round-bottom flask were added sulfoacetic acid (0.14g, 1.0 mmol), DMF (5 mL), HBTU (0.379g, 1 mmol), 3,5-dibromo-4-methylaniline (0.265g, 1 mmol), DIEA (0.52 mL, 3 mmol), and DMAP (0.012g, 0.1 mmol). The mixture was stirred at room temperature for 2 h, and then it was subjected to reversed-phase HPLC purification to give product L335-M34 as a white solid (0.385g, 99% yield):  $^1\text{H}$  NMR (500 MHz, DMSO)  $\delta$  10.08 (s, 1H), 7.87 (s, 2H), 3.52 (s, 2H), 2.42 (s, 3H);  $^{13}\text{C}$  NMR (DMSO)  $\delta$  164.6, 138.9, 130.5, 124.1, 121.8, 59.1, 22.6; ESI-HRMS calcd for  $\text{C}_9\text{H}_9\text{Br}_2\text{NO}_4\text{S}$  ( $\text{M} + \text{H}^+$ ) 385.8692, found 385.8696.

**Kinetic Analysis of mPTPA Inhibition.** The phosphatase activity of mPTPA was assayed using *p*-nitrophenyl phosphate (*p*NPP) as a substrate at 25 °C in 50 mM 3,3-dimethylglutarate buffer, pH 7.0, containing 1 mM EDTA with an ionic strength of 0.15 M adjusted by NaCl. The reaction was started by the addition of 50  $\mu\text{L}$  of the enzyme to 150  $\mu\text{L}$  of reaction mixture containing *p*NPP and various concentrations of the inhibitor in a 96-well plate. The final concentration for mPTPA was 5 nM. The final concentration for *p*NPP was 1 mM, which was the  $K_m$  value for mPTPA. The reaction was quenched after 15 min by the addition of 50  $\mu\text{L}$  of 5 N NaOH, and then 200  $\mu\text{L}$  of reaction mixture was transferred to a 96-well plate. The non-enzymatic hydrolysis of *p*NPP was corrected by measuring the control without the addition of enzyme. The amount of product *p*-nitrophenol was determined from the absorbance at 405 nm detected by a SpectraMax 384PLUS microplate spectrophotometer (Molecular Devices) using a molar extinction coefficient of 18 000  $\text{M}^{-1} \text{cm}^{-1}$ .  $\text{IC}_{50}$  values were calculated by fitting the absorbance at 405 nm versus inhibitor concentration to the following equation:

$$A_1/A_0 = \text{IC}_{50}/(\text{IC}_{50} + [\text{I}])$$

where  $A_1$  is the absorbance at 405 nm of the sample in the presence of inhibitor,  $A_0$  is the absorbance at 405 nm in the absence of inhibitor, and  $[\text{I}]$  is the concentration of the inhibitor.

For selectivity studies, the PTPs, including mPTPB, PTP1B, TC-PTP, SHP1, SHP2, FAP1, Lyp, PTP-MEG2, HePTP, PTPa, LAR, CD45, PTPg, VHR, Laforin, VHx, Cdc14A, and the low molecular weight PTP, were expressed and purified from *E. coli*. The final concentration for all PTPs was 5 nM. The inhibition assay for these PTPs was performed under the same conditions as mPTPA except using a different *p*NPP concentration corresponding to the  $K_m$  of the PTP studied. Inhibitor concentrations used for  $\text{IC}_{50}$  measurements cover the range from 0.2 to 5 $\times$  of the  $\text{IC}_{50}$  value.

**Mycobacterium tuberculosis Strains.** The Johns Hopkins Center for Tuberculosis Research laboratory reference strain Mtb H37Rv<sup>41</sup> was passaged twice through mice and frozen in aliquots at  $-80^\circ\text{C}$  before use. Aliquots were thawed and grown to logarithmic phase (optical density at 600 nm = 0.6) in Middlebrook 7H9 broth (Difco Laboratories, Detroit, MI) supplemented with 10% OADC (Becton Dickinson), 0.05% Tween, and 0.1% glycerol prior to aerosol infection.

**Animals.** Female guinea pigs ( $273 \pm 20.91$  g) with and without jugular vein catheters were purchased from Charles River Laboratories (Wilmington, MA). The animals were maintained under specific pathogen-free conditions and fed water and chow ad libitum. All procedures<sup>57</sup> followed protocols approved by the Institutional Animal Care and Use Committee at the Johns Hopkins University School of Medicine.

**In Vitro Anti-Mtb Assays. Alamar Blue Assay.** A colorimetric, microplate-based Alamar Blue assay (MABA) method was used to determine the MICs of mPTPA/B against *M. tuberculosis* isolates, as described earlier.<sup>58</sup> Briefly, cultures were incubated at 37 °C without shaking in 96-well plates. Alamar Blue reagent (Invitrogen) was added at 1:5 v/v prior to readout 24 h later using a Fluostar Optima fluorescence plate reader (BMG Labtech), equipped with a 544 nm excitation filter and a 590 nm emission filter.

**Macrophage Assays.** Inhibition of growth of *M. tuberculosis* (Erdman and H37Rv) in a macrophage cell culture was assessed as previously described.<sup>13</sup> Following activation with 50 U/mL IFN- $\gamma$  (Sigma, 087k1288), J774 macrophages were infected with *M. tuberculosis* strain at a multiplicity of infection of 1:1 for 1 h, washed, and incubated with 20  $\mu\text{g}/\text{mL}$  amikacin containing DMEM before adding the test compounds. Cells were washed and lysed, and different dilutions were plated on 7H11 agar plates. Colonies were counted after 3 weeks of incubation at 37 °C.

**Pharmacokinetics and Bioavailability Studies.** Separate groups of three catheterized guinea pigs each were given (i) a single dose of L01-Z08 at 20 mg/kg or L335-M34 at 50 mg/kg of body weight; (ii) L01-Z08 at 20 mg/kg and L335-M34 at 50 mg/kg were given together to test for possible drug–drug interactions that might alter the uptake and/or clearance of one or both of the compounds. All drugs were suspended in 1% DMSO, 0.5% DEA, 48.5% PEG 400, and 50% water. Blood was collected for analysis of these drugs in plasma predose and at 1, 4, 8, 24, and 48 h postdose. Plasma was separated and stored at  $-70^\circ\text{C}$  until analysis. Plasma drug concentrations were determined by liquid chromatography–mass spectrometry and liquid chromatography–tandem mass spectrometry over the concentration range of 0.005–1 mg/L with dilution to 10 mg/L. Pharmacokinetic variables were calculated from individual drug concentration–time data using noncompartmental methods as implemented in WinNonlin version 5.0 (Pharsight, Mountain View, CA) as described earlier.<sup>46,47</sup>

**Aerosol Infections.** Log-phase cultures of Mtb H37Rv were diluted 500-fold (to  $\sim 10^5$  bacilli/mL) in 1 $\times$  PBS for aerosol infection of guinea pigs. A total of 73 guinea pigs were aerosol-infected with a Madison chamber aerosol generation device (College of Engineering Shops, University of Wisconsin, Madison, WI) calibrated to deliver approximately  $10^2$  bacilli into guinea pig lungs, as previously described.<sup>43</sup>

**Antibiotic Treatment.** Beginning 28 days after aerosol infection, guinea pigs were randomized to different treatment and control groups. Guinea pigs were treated 5 days per week for 6 weeks at different dose ranges, as indicated in Table S1. Isoniazid (INH, H; Sigma), rifampicin (RIF, R; Sigma), and pyrazinamide (PZA, Z; Sigma) were dissolved in sterile distilled water. A cocktail solution of HRZ was prepared weekly and kept at 4 °C. Aarden compounds (L01-Z08 and L335-M34) were suspended in formulation and stored at room temperature for up to 1 week.

All animals were treated with a formulation consisting of 20% pumpkin (w/v) (Libby's 100% pure pumpkin) mixture

supplemented with Vitamin C (50 mg/kg mean body weight) and commercial lactobacillus (BD lactinex) (all purchased from Walmart, Towson, MD) to improve palatability and help stabilize the cecal flora, thereby preventing gastrointestinal dysbacteriosis or antibiotic-associated enteritis, as previously described.<sup>46,47</sup> Drug doses were administered in a final volume of 0.5 mL and were delivered in the posterior oropharynx by an automatic pipet with a disposable tip.

**Study End Points.** Guinea pigs were sacrificed on the day after aerosol infection (day 27), on the day of treatment initiation (day 0), and at the indicated time points after treatment to determine the numbers of CFU implanted in the lungs, pretreatment baseline CFU counts, and the post-treatment CFU counts, respectively.

Animal body weights were recorded on a weekly basis, and lung and spleen weights were recorded at the time of necropsy. The lungs of each animal were examined at necropsy for grossly visible lesions, and random samples from the left caudal lung lobe were dissected, placed into 10% buffered formaldehyde, and paraffin embedded for histopathological staining with hematoxylin and eosin (H&E). At least one entire H&E-stained cross section per animal lung (4 animals/group) was analyzed for degree of inflammation. The surface area occupied by granulomatous inflammation was determined by ImageJ software-based morphometry of digitized images of lung sections, and results are represented as percentage of lung surface area involved.<sup>47,59</sup>

The remaining lungs were homogenized in 10 mL of PBS, and homogenates were plated on 7H11 plates containing cycloheximide (50 mg/L), carbenicillin (100 mg/L), polymyxin B (200000 U/L), and trimethoprim (20 mg/L) and incubated for 28 days at 37 °C for CFU enumeration.

**Statistical Analysis.** CFU data were derived from 4–5 animals per group. Log-transformed CFU were used to calculate means and standard deviations. Comparisons of data among experimental groups were performed by Student's *t* test. Group means were compared by one-way analysis of variance (ANOVA) with Dunnett's post-test (D0 or untreated controls vs treatment groups) or Bonferroni comparison (all treatment groups), using GraphPad Prism version 4 (GraphPad, San Diego, CA). Values of *p* < 0.05 were considered to be statistically significant.

## ■ ASSOCIATED CONTENT

### ■ Supporting Information

The Supporting Information is available free of charge on the ACS Publications website at DOI: 10.1021/acsinfecdis.5b00133.

Figures S1–S3 (PDF)

## ■ AUTHOR INFORMATION

### Corresponding Author

\*Tel: (410) 502-8233. Fax: (410) 614-8173. E-mail: petros@jhmi.edu.

### Author Contributions

Experimental conception and design was by N.K.D., Z.Y.Z., F.B., and P.C.K. Data acquisition, analysis, and/or interpretation was by all authors. The manuscript was drafted by N.K.D., Z.Y.Z., and P.C.K. and approved by all authors.

## Notes

The authors declare the following competing financial interest(s): FB and ZYZ have ownership interests in Aarden Pharmaceuticals Inc.

## ■ ACKNOWLEDGMENTS

The authors thank Gregg Timony, Receptos, Inc., for WinNonlin analysis of pharmacokinetic data. This work was supported by National Institutes of Health and the National Institute of Allergy and Infectious Diseases, Phase I STTR No. 1R41H106123-01 to F.B., RO1 CA69202 to Z.Y.Z., and ACTG Grant 110007 and NIAID Grant UH2AI122309 to P.C.K. The content is solely the responsibility of the authors and does not necessarily represent the official views of the National Institutes of Health.

## ■ REFERENCES

- (1) Herbert, N., George, A., Baroness Masham of Ilton, Sharma, V., Oliver, M., Oxley, A., Raviglione, M., and Zumla, A. I. (2014) World TB Day 2014: finding the missing 3 million. *Lancet* 383, 1016–1018.
- (2) Lienhardt, C., Glaziou, P., Uplekar, M., Lonnroth, K., Getahun, H., and Raviglione, M. (2012) Global tuberculosis control: lessons learnt and future prospects. *Nat. Rev. Microbiol.* 10, 407–416.
- (3) Kempker, R. R., Kipiani, M., Mirtskhulava, V., Tukvadze, N., Magee, M. J., and Blumberg, H. M. (2015) Acquired Drug Resistance in Mycobacterium tuberculosis and Poor Outcomes among Patients with Multidrug-Resistant Tuberculosis. *Emerging Infect. Dis.* 21, 992–1001.
- (4) Zhang, Y. (2005) The magic bullets and tuberculosis drug targets. *Annu. Rev. Pharmacol. Toxicol.* 45, 529–564.
- (5) Clatworthy, A. E., Pierson, E., and Hung, D. T. (2007) Targeting virulence: a new paradigm for antimicrobial therapy. *Nat. Chem. Biol.* 3, 541–548.
- (6) Silva, A. P., and Taberner, L. (2010) New strategies in fighting TB: targeting Mycobacterium tuberculosis-secreted phosphatases MptpA & MptpB. *Future Med. Chem.* 2, 1325–1337.
- (7) Hunter, T. (1998) The Croonian Lecture 1997. The phosphorylation of proteins on tyrosine: its role in cell growth and disease. *Philos. Trans. R. Soc., B* 353, 583–605.
- (8) Beresford, N. J., Mulhearn, D., Szczepankiewicz, B., Liu, G., Johnson, M. E., Fordham-Skelton, A., Abad-Zapatero, C., Cavet, J. S., and Taberner, L. (2009) Inhibition of MptpB phosphatase from Mycobacterium tuberculosis impairs mycobacterial survival in macrophages. *J. Antimicrob. Chemother.* 63, 928–936.
- (9) He, R. J., Yu, Z. H., Zhang, R. Y., and Zhang, Z. Y. (2014) Protein tyrosine phosphatases as potential therapeutic targets. *Acta Pharmacol. Sin.* 35, 1227–1246.
- (10) Singh, R., Rao, V., Shakila, H., Gupta, R., Khera, A., Dhar, N., Singh, A., Koul, A., Singh, Y., Naseema, M., Narayanan, P. R., Paramasivan, C. N., Ramanathan, V. D., and Tyagi, A. K. (2003) Disruption of mptpB impairs the ability of Mycobacterium tuberculosis to survive in guinea pigs. *Mol. Microbiol.* 50, 751–762.
- (11) Singh, R., Singh, A., and Tyagi, A. K. (2005) Deciphering the genes involved in pathogenesis of Mycobacterium tuberculosis. *Tuberculosis* 85, 325–335.
- (12) Koul, A., Herget, T., Klebl, B., and Ullrich, A. (2004) Interplay between mycobacteria and host signalling pathways. *Nat. Rev. Microbiol.* 2, 189–202.
- (13) Zhou, B., He, Y., Zhang, X., Xu, J., Luo, Y., Wang, Y., Franzblau, S. G., Yang, Z., Chan, R. J., Liu, Y., Zheng, J., and Zhang, Z. Y. (2010) Targeting mycobacterium protein tyrosine phosphatase B for antituberculosis agents. *Proc. Natl. Acad. Sci. U. S. A.* 107, 4573–4578.
- (14) Castandet, J., Prost, J. F., Peyron, P., Astarie-Dequeker, C., Anes, E., Cozzone, A. J., Griffiths, G., and Maridonneau-Parini, I. (2005) Tyrosine phosphatase MptpA of Mycobacterium tuberculosis inhibits phagocytosis and increases actin polymerization in macrophages. *Res. Microbiol.* 156, 1005–1013.



- (15) Chauhan, P., Reddy, P. V., Singh, R., Jaisinghani, N., Gandotra, S., and Tyagi, A. K. (2013) Secretory phosphatases deficient mutant of *Mycobacterium tuberculosis* imparts protection at the primary site of infection in guinea pigs. *PLoS One* 8, e77930.
- (16) Bach, H., Papavinasasundaram, K. G., Wong, D., Hmama, Z., and Av-Gay, Y. (2008) *Mycobacterium tuberculosis* virulence is mediated by PtpA dephosphorylation of human vacuolar protein sorting 33B. *Cell Host Microbe* 3, 316–322.
- (17) Wong, D., Bach, H., Sun, J., Hmama, Z., and Av-Gay, Y. (2011) *Mycobacterium tuberculosis* protein tyrosine phosphatase (PtpA) excludes host vacuolar-H<sup>+</sup>-ATPase to inhibit phagosome acidification. *Proc. Natl. Acad. Sci. U. S. A.* 108, 19371–19376.
- (18) Cowley, S. C., Babakaiff, R., and Av-Gay, Y. (2002) Expression and localization of the *Mycobacterium tuberculosis* protein tyrosine phosphatase PtpA. *Res. Microbiol.* 153, 233–241.
- (19) Zeng, L. F., Xu, J., He, Y., He, R., Wu, L., Gunawan, A. M., and Zhang, Z. Y. (2013) A facile hydroxyindole carboxylic acid based focused library approach for potent and selective inhibitors of *Mycobacterium* protein tyrosine phosphatase B. *ChemMedChem* 8, 904–908.
- (20) He, Y., Xu, J., Yu, Z. H., Gunawan, A. M., Wu, L., Wang, L., and Zhang, Z. Y. (2013) Discovery and evaluation of novel inhibitors of *mycobacterium* protein tyrosine phosphatase B from the 6-Hydroxy-benzofuran-S-carboxylic acid scaffold. *J. Med. Chem.* 56, 832–842.
- (21) He, R., Zeng, L. F., He, Y., Zhang, S., and Zhang, Z. Y. (2013) Small molecule tools for functional interrogation of protein tyrosine phosphatases. *FEBS J.* 280, 731–750.
- (22) Puius, Y. A., Zhao, Y., Sullivan, M., Lawrence, D. S., Almo, S. C., and Zhang, Z. Y. (1997) Identification of a second aryl phosphate-binding site in protein-tyrosine phosphatase 1B: a paradigm for inhibitor design. *Proc. Natl. Acad. Sci. U. S. A.* 94, 13420–13425.
- (23) He, R., Yu, Z. H., Zhang, R. Y., Wu, L., Gunawan, A. M., Lane, B. S., Shim, J. S., Zeng, L. F., He, Y., Chen, L., Wells, C. D., Liu, J. O., and Zhang, Z. Y. (2015) Exploring the Existing Drug Space for Novel pTyr Mimetic and SHP2 Inhibitors. *ACS Med. Chem. Lett.* 6, 782–786.
- (24) Manger, M., Scheck, M., Prinz, H., von Kries, J. P., Langer, T., Saxena, K., Schwalbe, H., Furstner, A., Rademann, J., and Waldmann, H. (2005) Discovery of *Mycobacterium tuberculosis* protein tyrosine phosphatase A (MptpA) inhibitors based on natural products and a fragment-based approach. *ChemBioChem* 6, 1749–1753.
- (25) Rawls, K. A., Lang, P. T., Takeuchi, J., Imamura, S., Baguley, T. D., Grundner, C., Alber, T., and Ellman, J. A. (2009) Fragment-based discovery of selective inhibitors of the *Mycobacterium tuberculosis* protein tyrosine phosphatase PtpA. *Bioorg. Med. Chem. Lett.* 19, 6851–6854.
- (26) Chandra, K., Dutta, D., Das, A. K., and Basak, A. (2010) Design, synthesis and inhibition activity of novel cyclic peptides against protein tyrosine phosphatase A from *Mycobacterium tuberculosis*. *Bioorg. Med. Chem.* 18, 8365–8373.
- (27) Chiaradia, L. D., Martins, P. G., Cordeiro, M. N., Guido, R. V., Ecco, G., Andricopulo, A. D., Yunes, R. A., Vernal, J., Nunes, R. J., and Terenzi, H. (2012) Synthesis, biological evaluation, and molecular modeling of chalcone derivatives as potent inhibitors of *Mycobacterium tuberculosis* protein tyrosine phosphatases (PtpA and PtpB). *J. Med. Chem.* 55, 390–402.
- (28) He, Y., Zeng, L. F., Yu, Z. H., He, R., Liu, S., and Zhang, Z. Y. (2012) Bicyclic benzofuran and indole-based salicylic acids as protein tyrosine phosphatase inhibitors. *Bioorg. Med. Chem.* 20, 1940–1946.
- (29) Moreira, W., Ngan, G. J., Low, J. L., Poulsen, A., Chia, B. C., Ang, M. J., Yap, A., Fulwood, J., Lakshmanan, U., Lim, J., Khoo, A. Y., Flotow, H., Hill, J., Raju, R. M., Rubin, E. J., and Dick, T. (2015) Target mechanism-based whole-cell screening identifies bortezomib as an inhibitor of caseinolytic protease in mycobacteria. *mBio* 6, e00253-15.
- (30) Cole, S. T., Brosch, R., Parkhill, J., Garnier, T., Churcher, C., Harris, D., Gordon, S. V., Eiglmeier, K., Gas, S., Barry, C. E., 3rd, Tekai, F., Badcock, K., Basham, D., Brown, D., Chillingworth, T., Connor, R., Davies, R., Devlin, K., Feltwell, T., Gentles, S., Hamlin, N., Holroyd, S., Hornsby, T., Jagels, K., Krogh, A., McLean, J., Moule, S., Murphy, L., Oliver, K., Osborne, J., Quail, M. A., Rajandream, M. A., Rogers, J., Rutter, S., Seeger, K., Skelton, J., Squares, R., Squares, S., Sulston, J. E., Taylor, K., Whitehead, S., and Barrell, B. G. (1998) Deciphering the biology of *Mycobacterium tuberculosis* from the complete genome sequence. *Nature* 393, 537–544.
- (31) Janne, P. A., Gray, N., and Settleman, J. (2009) Factors underlying sensitivity of cancers to small-molecule kinase inhibitors. *Nat. Rev. Drug Discovery* 8, 709–723.
- (32) Andersen, J. N., Jansen, P. G., Echwald, S. M., Mortensen, O. H., Fukada, T., Del Vecchio, R., Tonks, N. K., and Moller, N. P. (2004) A genomic perspective on protein tyrosine phosphatases: gene structure, pseudogenes, and genetic disease linkage. *FASEB J.* 18, 8–30.
- (33) Arena, S., Benvenuti, S., and Bardelli, A. (2005) Genetic analysis of the kinome and phosphatome in cancer. *Cell. Mol. Life Sci.* 62, 2092–2099.
- (34) Barr, A. J. (2010) Protein tyrosine phosphatases as drug targets: strategies and challenges of inhibitor development. *Future Med. Chem.* 2, 1563–1576.
- (35) Poirier, V., Bach, H., and Av-Gay, Y. (2014) *Mycobacterium tuberculosis* promotes anti-apoptotic activity of the macrophage by PtpA protein-dependent dephosphorylation of host GSK3 $\alpha$ . *J. Biol. Chem.* 289, 29376–29385.
- (36) Pizarro-Cerda, J., and Cossart, P. (2004) Subversion of phosphoinositide metabolism by intracellular bacterial pathogens. *Nat. Cell Biol.* 6, 1026–1033.
- (37) Grundner, C., Cox, J. S., and Alber, T. (2008) Protein tyrosine phosphatase PtpA is not required for *Mycobacterium tuberculosis* growth in mice. *FEMS Microbiol. Lett.* 287, 181–184.
- (38) De Groote, M. A., Gilliland, J. C., Wells, C. L., Brooks, E. J., Woolhiser, L. K., Gruppo, V., Peloquin, C. A., Orme, I. M., and Lenaerts, A. J. (2011) Comparative studies evaluating mouse models used for efficacy testing of experimental drugs against *Mycobacterium tuberculosis*. *Antimicrob. Agents Chemother.* 55, 1237–1247.
- (39) Gillespie, S. H., Crook, A. M., McHugh, T. D., Mendel, C. M., Meredith, S. K., Murray, S. R., Pappas, F., Phillips, P. P., and Nunn, A. J. (2014) Four-month moxifloxacin-based regimens for drug-sensitive tuberculosis. *N. Engl. J. Med.* 371, 1577–1587.
- (40) Mitchison, D. A., and Chang, K. C. (2009) Experimental Models of Tuberculosis: Can We Trust the Mouse? *Am. J. Respir. Crit. Care Med.* 180, 201–202.
- (41) Ahmad, Z., Fraig, M. M., Bisson, G. P., Nuermberger, E. L., Grosset, J. H., and Karakousis, P. C. (2011) Dose-dependent activity of pyrazinamide in animal models of intracellular and extracellular tuberculosis infections. *Antimicrob. Agents Chemother.* 55, 1527–1532.
- (42) Ahmad, Z., Fraig, M. M., Pinn, M. L., Tyagi, S., Nuermberger, E. L., Grosset, J. H., and Karakousis, P. C. (2011) Effectiveness of tuberculosis chemotherapy correlates with resistance to *Mycobacterium tuberculosis* infection in animal models. *J. Antimicrob. Chemother.* 66, 1560–1566.
- (43) Ahmad, Z., Klinkenberg, L. G., Pinn, M. L., Fraig, M. M., Peloquin, C. A., Bishai, W. R., Nuermberger, E. L., Grosset, J. H., and Karakousis, P. C. (2009) Biphasic kill curve of isoniazid reveals the presence of drug-tolerant, not drug-resistant, *Mycobacterium tuberculosis* in the guinea pig. *J. Infect. Dis.* 200, 1136–1143.
- (44) Ahmad, Z., Nuermberger, E. L., Tasneen, R., Pinn, M. L., Williams, K. N., Peloquin, C. A., Grosset, J. H., and Karakousis, P. C. (2010) Comparison of the 'Denver regimen' against acute tuberculosis in the mouse and guinea pig. *J. Antimicrob. Chemother.* 65, 729–734.
- (45) Ahmad, Z., Pinn, M. L., Nuermberger, E. L., Peloquin, C. A., Grosset, J. H., and Karakousis, P. C. (2010) The potent bactericidal activity of streptomycin in the guinea pig model of tuberculosis ceases due to the presence of persisters. *J. Antimicrob. Chemother.* 65, 2172–2175.
- (46) Dutta, N. K., Alsultan, A., Gniadek, T. J., Belchis, D. A., Pinn, M. L., Mdluli, K. E., Nuermberger, E. L., Peloquin, C. A., and Karakousis, P. C. (2013) Potent rifamycin-sparing regimen cures guinea pig tuberculosis as rapidly as the standard regimen. *Antimicrob. Agents Chemother.* 57, 3910–3916.



- (47) Dutta, N. K., Illei, P. B., Peloquin, C. A., Pinn, M. L., Mdluli, K. E., Nuermberger, E. L., Grosset, J. H., and Karakousis, P. C. (2012) Rifapentine is not more active than rifampin against chronic tuberculosis in guinea pigs. *Antimicrob. Agents Chemother.* 56, 3726–3731.
- (48) Dutta, N. K., Pinn, M. L., Zhao, M., Rudek, M. A., and Karakousis, P. C. (2013) Thioridazine lacks bactericidal activity in an animal model of extracellular tuberculosis. *J. Antimicrob. Chemother.* 68, 1327–1330.
- (49) Flynn, J., and Chan, J. (2004) Animal models of tuberculosis, in *Tuberculosis* (Rom, W., and Garay, S., Eds.) 2nd ed., pp 237–250, Lippincott Williams & Wilkins, Philadelphia, PA.
- (50) Lenaerts, A. J., Hoff, D., Aly, S., Ehlers, S., Andries, K., Cantarero, L., Orme, I. M., and Basaraba, R. J. (2007) Location of persisting mycobacteria in a Guinea pig model of tuberculosis revealed by r207910. *Antimicrob. Agents Chemother.* 51, 3338–3345.
- (51) Tsai, M. C., Chakravarty, S., Zhu, G., Xu, J., Tanaka, K., Koch, C., Tufariello, J., Flynn, J., and Chan, J. (2006) Characterization of the tuberculous granuloma in murine and human lungs: cellular composition and relative tissue oxygen tension. *Cell. Microbiol.* 8, 218–232.
- (52) Aly, S., Wagner, K., Keller, C., Malm, S., Malzan, A., Brandau, S., Bange, F. C., and Ehlers, S. (2006) Oxygen status of lung granulomas in *Mycobacterium tuberculosis*-infected mice. *J. Pathol.* 210, 298–305.
- (53) Dutta, N. K., and Karakousis, P. C. (2014) Latent tuberculosis infection: myths, models, and molecular mechanisms. *Microbiol. Mol. Biol. Rev.* 78, 343–371.
- (54) Dorman, S. E., Goldberg, S., Stout, J. E., Muzanyi, G., Johnson, J. L., Weiner, M., Bozeman, L., Heilig, C. M., Feng, P. J., Moro, R., Narita, M., Nahid, P., Ray, S., Bates, E., Haile, B., Nuermberger, E. L., Vernon, A., and Schluger, N. W. (2012) Substitution of rifapentine for rifampin during intensive phase treatment of pulmonary tuberculosis: study 29 of the tuberculosis trials consortium. *J. Infect. Dis.* 206, 1030–1040.
- (55) Prideaux, B., Via, L. E., Zimmerman, M. D., Eum, S., Sarathy, J., O'Brien, P., Chen, C., Kaya, F., Weiner, D. M., Chen, P. Y., Song, T., Lee, M., Shim, T. S., Cho, J. S., Kim, W., Cho, S. N., Olivier, K. N., Barry, C. E., 3rd, and Dartois, V. (2015) The association between sterilizing activity and drug distribution into tuberculosis lesions. *Nat. Med.* 21, 1223–1227.
- (56) Via, L. E., Savic, R., Weiner, D. M., Zimmerman, M. D., Prideaux, B., Irwin, S. M., Lyon, E., O'Brien, P., Gopal, P., Eum, S., Lee, M., Lanoix, J. P., Dutta, N. K., Shim, T., Cho, J. S., Kim, W., Karakousis, P. C., Lenaerts, A., Nuermberger, E., Barry, C. E., 3rd, and Dartois, V. (2015) Host-Mediated Bioactivation of Pyrazinamide: Implications for Efficacy, Resistance, and Therapeutic Alternatives. *ACS Infect. Dis.* 1, 203–214.
- (57) Klinkenberg, L. G., Sutherland, L. A., Bishai, W. R., and Karakousis, P. C. (2008) Metronidazole lacks activity against *Mycobacterium tuberculosis* in an in vivo hypoxic granuloma model of latency. *J. Infect. Dis.* 198, 275–283.
- (58) Franzblau, S. G., Witzig, R. S., McLaughlin, J. C., Torres, P., Madico, G., Hernandez, A., Degnan, M. T., Cook, M. B., Quenzer, V. K., Ferguson, R. M., and Gilman, R. H. (1998) Rapid, low-technology MIC determination with clinical *Mycobacterium tuberculosis* isolates by using the microplate Alamar Blue assay. *Journal of clinical microbiology* 36, 362–366.
- (59) Dutta, N. K., Alsultan, A., Peloquin, C. A., and Karakousis, P. C. (2013) Preliminary pharmacokinetic study of repeated doses of rifampin and rifapentine in guinea pigs. *Antimicrob. Agents Chemother.* 57, 1535–1537.